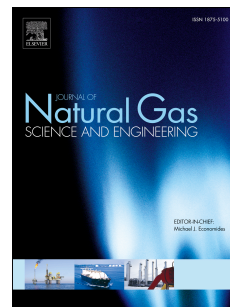


Accepted Manuscript

Novel integrated techniques of drilling–slotting–separation–sealing for enhanced coal bed methane recovery in underground coal mines

Quanle Zou, Baiquan Lin, Chunshan Zheng, Zhiyong Hao, Cheng Zhai, Ting Liu, Jinyan Liang, Fazhi Yan, Wei Yang, Chuanjie Zhu



PII: S1875-5100(15)30054-8

DOI: [10.1016/j.jngse.2015.07.033](https://doi.org/10.1016/j.jngse.2015.07.033)

Reference: JNGSE 891

To appear in: *Journal of Natural Gas Science and Engineering*

Received Date: 26 May 2015

Revised Date: 19 July 2015

Accepted Date: 20 July 2015

Please cite this article as: Zou, Q., Lin, B., Zheng, C., Hao, Z., Zhai, C., Liu, T., Liang, J., Yan, F., Yang, W., Zhu, C., Novel integrated techniques of drilling–slotting–separation–sealing for enhanced coal bed methane recovery in underground coal mines, *Journal of Natural Gas Science & Engineering* (2015), doi: 10.1016/j.jngse.2015.07.033.

This is a PDF file of an unedited manuscript that has been accepted for publication. As a service to our customers we are providing this early version of the manuscript. The manuscript will undergo copyediting, typesetting, and review of the resulting proof before it is published in its final form. Please note that during the production process errors may be discovered which could affect the content, and all legal disclaimers that apply to the journal pertain.

*Corresponding author.

E-mail address: 15262143114@139.com (B. Lin)

Novel integrated techniques of drilling–slotting–separation–sealing for enhanced coal bed methane recovery in underground coal mines

Quanle Zou^{a,b}; Baiquan Lin^{a,b*}; Chunshan Zheng^c; Zhiyong Hao^{a,b}; Cheng Zhai^{a,b}; Ting Liu^{a,b}; Jinyan Liang^d;
Fazhi Yan^{a,b}; Wei Yang^{a,b}; Chuanjie Zhu^{a,b}

^a School of Safety Engineering, China University of Mining & Technology, Xuzhou 221116, P.R.China

^b State Key Laboratory of Coal Resources and Safe Mining, Xuzhou 221116, P.R.China

^c School of Mechanical and Mining Engineering, the University of Queensland, QLD 4072, Australia

^d Department of Safety Engineering, Xuzhou Higher Occupation School of Mechanical and Electrical Engineering in Jiangsu Province, Xuzhou 320305, P.R.China

Abstract Coal bed Methane (CBM), a primary component of natural gas, is a relatively clean source of energy. Nevertheless, the impact of considerable coal mine methane emission on climate change in China has gained an increasing attention as coal production has powered the country's economic development. It is well-known that coal bed methane is a typical greenhouse gas, the greenhouse effect index of which is 30 times larger than that of carbon dioxide. Besides, gas disasters such as gas explosive and outburst, *etc.* pose a great threat to the safety of miners. Therefore, measures must be taken to capture coal mine methane before mining. This helps to enhance safety during mining and extract an environmentally friendly gas as well. However, as a majority of coal seams in China have low-permeability, it is difficult to achieve efficient methane drainage. Enhancing coal permeability is a good choice for high-efficiency drainage of coal mine methane. In this paper, a modified coal-methane co-exploitation model was established and a combination of drilling–slotting–separation–sealing was proposed to enhance coal permeability and CBM recovery. Firstly, rapid drilling assisted by water-jet and significant permeability enhancement via pressure relief were investigated, guiding the fracture network formation around borehole for high efficient gas flow. Secondly, based on the principle of swirl separation, the coal–water–gas separation instrument was developed to eliminate the risk of gas accumulation during slotting and reduce the gas emission from the ventilation air. Thirdly, to improve the performance of sealing material, we developed a novel cement-based composite sealing material based on the microcapsule technique. Additionally, a novel sealing–isolation combination technique was also proposed. Results of field test indicate that gas concentration in slotted boreholes is 1.05–1.91 times higher than that in conventional boreholes. Thus, the proposed novel integrated techniques achieve the goal of high-efficiency coal bed methane recovery.

Keywords: Enhanced coal bed methane recovery; Permeability enhancement; Dual-power drilling; Sealing material; Coal-water-gas separation

1. Introduction

It has been widely accepted that emissions of greenhouse gases (GHGs) are the primary contributor to anthropogenic climate change (Lashof and Ahuja, 1990; Hook and Tang, 2013). The atmospheric concentration of methane (CH₄) has increased to 1803 ppb by 2012, which is 2.5 times larger than the pre-industrial level

(Bamberger et al., 2014; Li et al., 2015b). In general, atmospheric methane originates from both anthropogenic and natural activities (Al-Amin and Kari, 2013; Warmuzinski et al., 2008; Su et al., 2005,2011). Among the various anthropogenic sources, methane emission from coal mining accounts for 8.9-12.8% (Cheng et al., 2011; Yusuf et al., 2012). It is estimated that coal mine methane (CMM) emission would increase to 793 MtCO₂e by 2020 (IPCC, 2007). Approximately 85-90% of the total CMM emission comes from underground coal mines, a majority of which is from drainage systems and ventilation air (Karakurt et al. 2011; Baris, 2013). Therefore, it is of crucial significance to develop corresponding techniques to reduce such high amounts of coal bed methane emission.

Since adopting the Policy of Reform and Opening-Up to the outside world in 1978, China has not only achieved exceptionally rapid economic growth but also became the 'workshop of the world' (Li et al., 2015b). The primary, secondary and tertiary industries account for 9.2%, 42.6% and 48.2% of China's GDP in 2014, respectively. This industrial structure relies on an adequate supply of affordable energy consequentially. China's total proved coal, oil and natural gas reserves are 114.5 billion tons, 2.5 billion tons and 33 trillion cubic metres, respectively, indicating that its energy structure is characterised by rich coal reserve, and meagre oil and gas reserves (BP, 2014). Coal accounts for approximately 70% of Chinese primary energy consumption in a long term. Chinese coal production and consumption constituted 47.5% and 52% of total worldwide coal production and consumption in 2013, respectively (Nejat et al., 2015). At present, China is the world's largest coal producer and consumer (Shealy and Dorian, 2010; Zhao and Chen, 2014).

As shallow coal reserves in China have been exhausted by a rapid coal-production rate, coal mining level is deepening at an annual rate of 10 - 20 m (He and Li, 2012). As a result, the high gas pressure and gas content in coal seams are becoming a key constraint on the deep high-efficiency coal mining in China (Li et al., 2015a; Ni et al., 2014; Wang et al., 2014; Liu et al., 2014c). Gas drainage is an effective measure to solve the aforementioned problem. The main benefits of gas drainage in gas-rich coal seams are as follows: decreased environmental impact, an improvement in the health and safety of underground workforce and the production of a relatively clean source of energy (Wang et al., 2012a; Yan et al., 2015). However, the permeability of coal seams in China is universally low. As shown in Fig. 1, the permeability coefficients of Chinese raw coal seams are four orders of magnitude lower than that of American coal seams. From a geological viewpoint, a majority of coal seams in China took shape over the Carboniferous-Permian period, during which the coal suffered from strong tectonic movements and its original cracks were destroyed. Consequently, the coal structure became soft and complicated, which is not conducive to gas flow (Pan et al., 2015). CMM in China is characterised by poor drainage performance (Lin et al., 2014; Hao et al., 2014). Therefore, measures should be taken to enhance the permeability of the high gassy and low-permeability coal seams.

Carbon dioxide capture and storage (CCS) technologies involve capturing CO₂ from anthropogenic sources, depositing it in suitable deep geological formations and isolating the gas from the atmosphere (Mazzotti et al., 2009; Budzianowski, 2012,2013). This is an effective and vital option for atmospheric CO₂ concentration control and climate change mitigation, which attributes to the continued utilisation of fossil fuels. Recently, the techniques for enhanced coal bed methane (ECBM) recovery have attracted wide attention. The enhanced gas recovery (EGR) technology using CO₂ injection was considered as a promising measure for realising the design of efficient null-greenhouse-gas-emission power plants fuelled by CBM extracted from deep coal seams (Gunter et al., 1997;

Rodrigues et al., 2013). Once injected into coal seams with sealing cap rock, CO₂ is adsorbed and retained permanently. Meanwhile, the injected CO₂ will displace coal bed methane owing to its higher affinity for coal, thereby enhancing the primary recovery of methane. Substantial research has been conducted to evaluate the storage capacity of coal seams (Saghafi, 2010; Pan and Connell, 2011), understand adsorption/desorption dynamics during injection (Li et al., 2014a; Yu et al., 2014; Liu et al., 2014d) and characterise coal swelling and permeability (Mazumder and Wolf, 2008; Kiyama et al., 2011; Qu et al., 2012). These investigations provide the experimental and theoretical basis for field tests and future commercial deployment of CO₂-related enhanced coal bed methane (CO₂-ECBM) recovery (Qin, 2008; White et al., 2005). Obviously, this technique is not suitable for exploitation of deep high gassy and low-permeability coal seams due to the fact that the risk of coal and gas outbursts still exists after adopting this method (Lama and Bodziony, 1998; Sobczyk, 2014). Several hydraulic techniques have been proposed to solve the aforementioned problem (Liu et al., 2014, 2015; Li et al., 2015; Yan et al., 2015; Wang et al., 2014b; Wang et al., 2015). In this paper, novel integrated techniques of drilling–slotting–separation–sealing were elaborated. Initially, a modified coal-methane co-exploitation model was proposed. Based on the model, the proposed techniques were introduced via the following three methods: drilling–slotting integrated technique, coal–water–gas separation technique and sealing–isolation combination technique. Finally, field tests were conducted. The proposed techniques could significantly enhance coal bed methane recovery and substantially reduce the coal mine methane emission from drainage system and ventilation air, which makes them viable and highly efficient methods for the exploitation of deep coal seam with low permeability and high gas content.

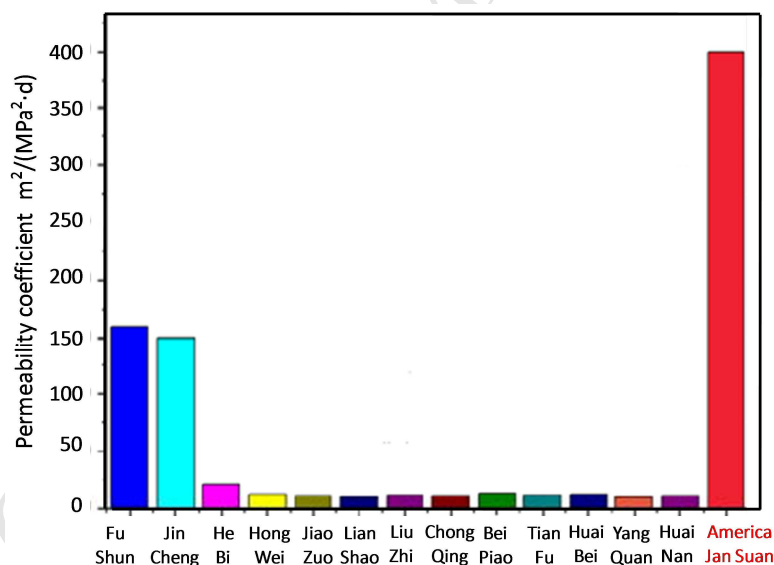


Fig. 1. Comparisons of permeability coefficients of raw coal seam in typical coal mines in China with those in America

2. A modified coal–methane co-exploitation model

Coal and methane are two kinds of resources in a gas-rich coal seam (Karacan et al., 2011). If methane resource only is exploited, it is difficult to drain coal bed methane. Likewise, if coal resource only is exploited, there is a risk of gas explosion and outburst due to the high gas concentration in coal seams. Moreover, the emission of methane into the atmosphere could have a serious impact on climate change (Sander and Connell, 2012, 2014). Therefore, a coal–methane co-exploitation model was established by Wang and Cheng (2012b) to

solve the aforementioned dilemma. In this model, a coal seam with relatively lower gas risks is selected as an initial mining coal seam (Fig. 2). Upon mining this coal seam, the gas pressure in the adjacent coal seams (top and below) are relieved, thereby increasing coal permeability, which facilitates high-efficiency methane drainage. Adjacent coal seams could become less gas-rich with the help of effective methane drainage, and thus, both coal and methane could be exploited simultaneously in a safe environment (Liu et al., 2013; Zhou et al., 2015). The proposed coal-methane co-exploitation model could solve the gas problems in multiple coal seam mining and recover coal bed methane, thereby reducing the GHGs emissions. However, the high efficiency and safe mining in the initial coal seam under the gas-rich and low permeability condition is not taken into consideration in this model, i.e., there exists no coal seam with acceptable gas risks in multi-seam mining. Moreover, if the distances between the initial and adjacent coal seam are so large that the exploitation of initial coal seam cannot fully relieve the pressure of adjacent coal seams. Thus, a modified coal-methane co-exploitation model was put forward (Fig. 3). In the modified model, the integrated techniques of drilling–slotting–separation–sealing is adopted to reduce the gas content and eliminate the risk of gas burst in the initial/adjacent coal seam. As a result, high-efficiency production and mining safety are achieved in both the initial and adjacent coal seams. The pressure relief of adjacent coal seam through the initial coal seam has been investigated in detail and the related techniques are relatively mature (Yang et al., 2011a,b, 2014; Zhou et al., 2015; Liu et al., 2013; Suchowerska, et al., 2013; Guo et al., 2012). In this study, we introduce novel integrated techniques involving drilling–slotting–separation–sealing (Fig. 4). The techniques, aiming at achieving high efficiency and safe mining in the initial coal seam, are composed of the following three key steps: drilling–slotting integrated technique, coal–water–gas separation technique and sealing–isolation combination technique. Correspondingly, the instruments for dual-power drilling (used before slotting) and coal–water–gas separation (used during slotting) are developed. Besides, the novel sealing material (used after slotting) and related instruments are also developed for effective sealing. Those aforementioned techniques are elaborated in following sections.

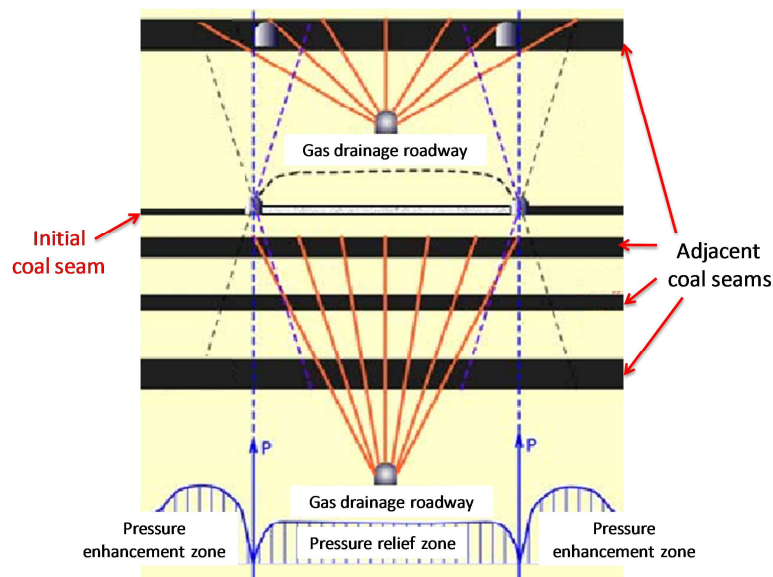


Fig. 2. A schematic diagram of coal and gas exploitation for multiple gas-rich coal seams (Yuan et al., 2009)

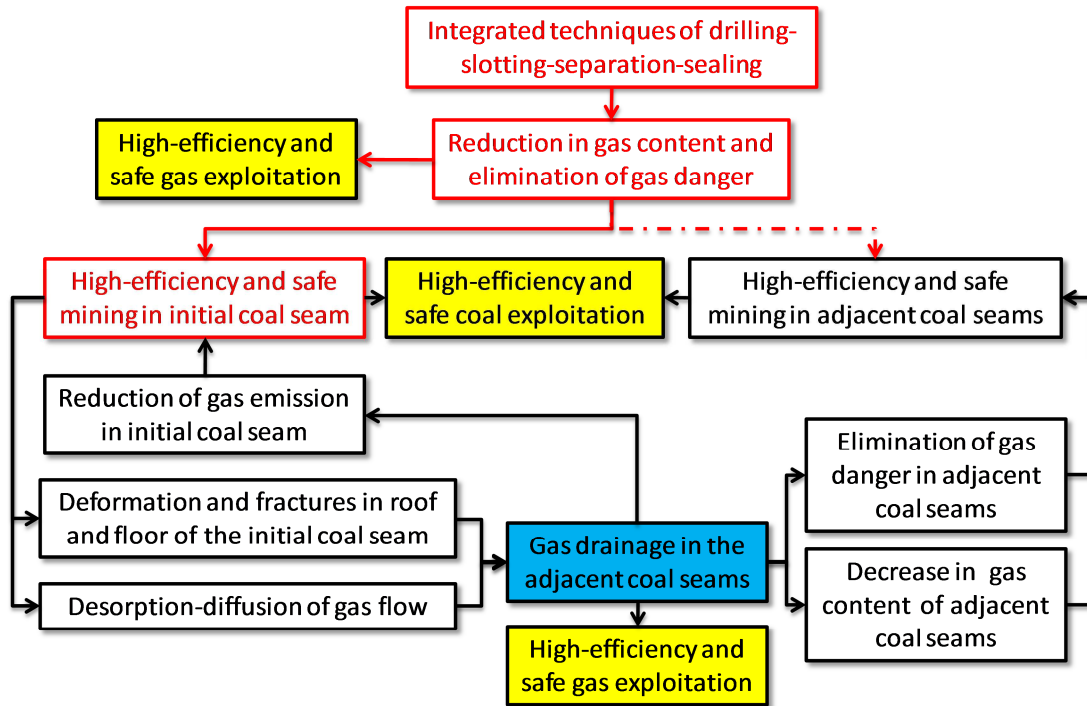


Fig. 3. A modified coal–methane co-exploitation model for coal-rich coal seams

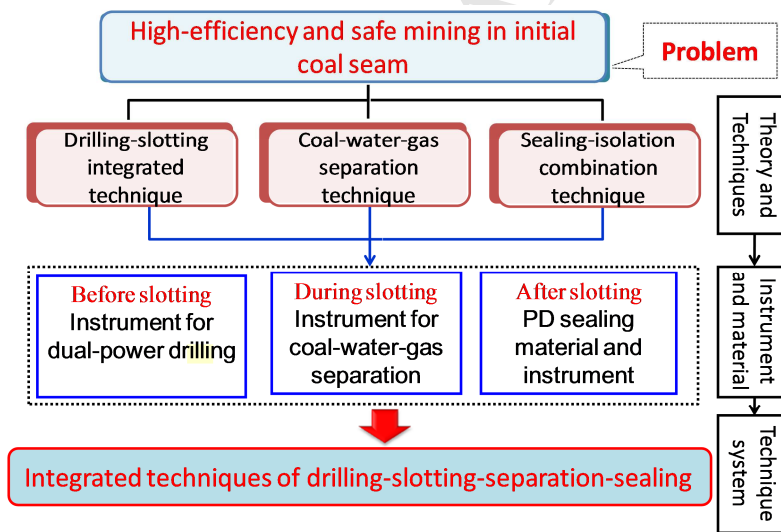


Fig. 4. A Schematic diagram of the proposed novel integrated technique including drilling, slotting and sealing

3. Drilling–slotting integrated technique

3.1. Steps involved in drilling–slotting

The drilling–slotting integrated technique is an organic combination of mechanical drilling and water-jet slotting. As shown in Fig. 5, the procedures of this technique can be summarised as follows: The coal is broken and an advanced weakening zone on the coal surface is formed via water-jet impact. The strength of coal in this zone lowers significantly (Sitharam 1999; Yin et al., 2015). Subsequently, the coal can be easily crushed by a mechanical blade. When the mechanical drill reaches the pre-determined location, the drill pipe is pulled outwards and several slots around borehole are cut by using high-pressure water jet.

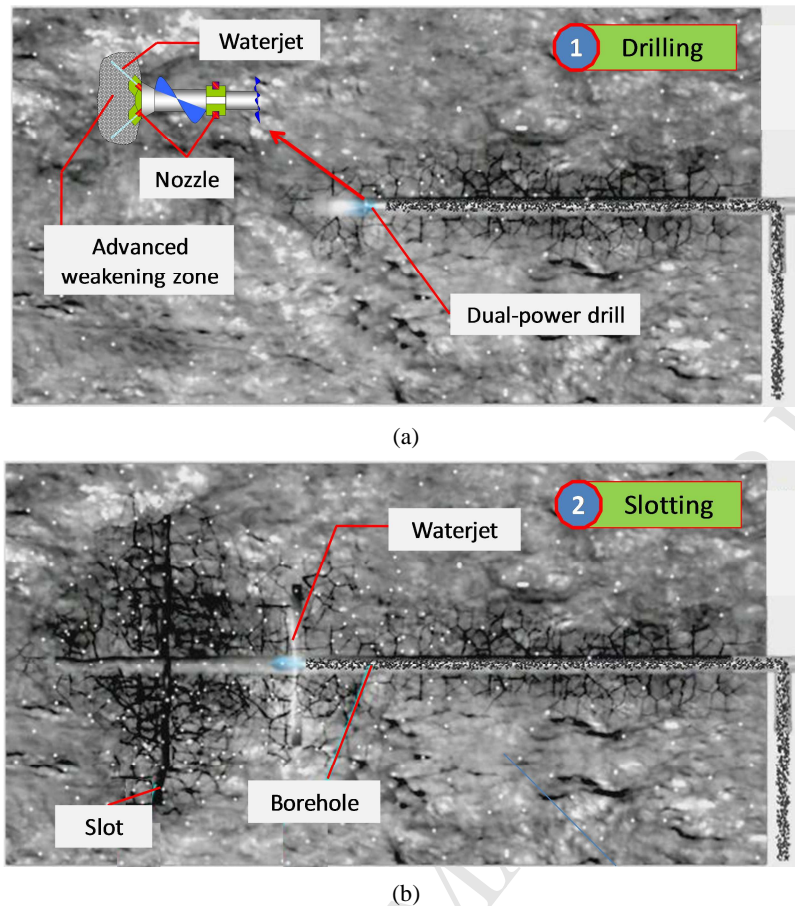


Fig. 5. Steps involved in the drilling–slotting integrated technique. (a) Drilling with the combination of high-pressure water jet and mechanical drill. (b) Cutting slots on the coal seam using the high-pressure water jet.

3.2. Dual-power drilling

The dual-power drill (Fig. 6a, b) plays a crucial role in the process of drilling and slotting, which works via the cooperation of the mechanical blade, nozzles, springs and solid plastic balls. When the water with relatively low-pressure flows into the drill, spring 1 and spring 2 are compressed. The water is ejected out through nozzle 1 and nozzle 2, which is conducive to the rapid drilling. If the pressure of water is over a critical value, spring 1 is fully compressed and all the water is ejected out through nozzle 2, which contributes to the effective slotting. In most cases, the convergent–straight nozzle (Figure 6c) is used (Lu et al., 2010). In Fig. 6, α is the convergence angle, S is the length of convergence, L is the length of outlet cylinder and d is the outlet diameter.

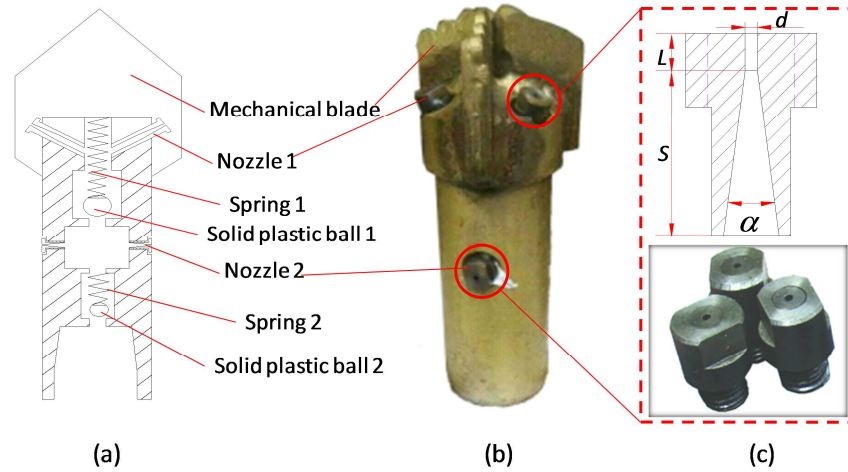


Fig. 6. Dual-power drill. (a) Cross-sectional diagram. (b) Physical map. (c) Nozzle. The top figure is its cross-sectional diagram and the bottom one is the physic map.

Pictures in Fig. 7 show the comparison of boreholes drilled by conventional drilling and dual-power drilling. The mass ratio of the crushed coal, cement and gypsum in the specimens is 1:35:35 (Huang et al., 2011). The size of the specimens is $1\text{ m} \times 1\text{ m} \times 1\text{ m}$. The compressive strength and elasticity modulus are 12.4 MPa and 1.5 GPa. The pump pressure is 20 MPa. It can be seen in Fig. 7 that the diameter of the borehole enlarges significantly, which is conducive to the timely discharge of the crushed coal. During dual-power drilling, an inverted cone-shaped coal pillar is formed. The elimination of coal pillar's confining pressure is attributed to the reduction in yield stress (Chen et al., 2015; Yin et al., 2015). Thus, this rock pillar is easily broken by a mechanical drill, which substantially increases the drilling velocity.

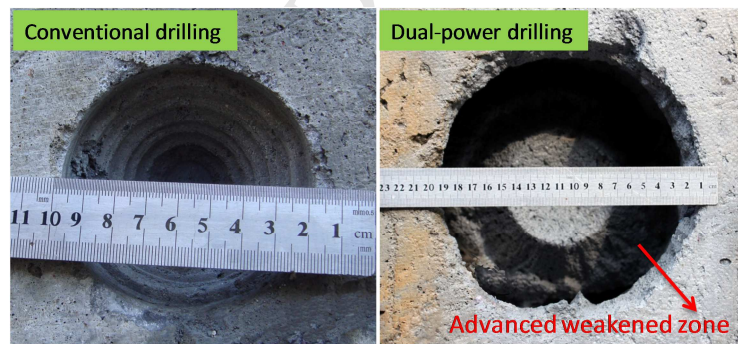


Fig. 7. Comparison of drilling effect of conventional drilling and dual-power drilling

An advanced weakened zone is the key factor in achieving successful results with dual-power drilling, the formation of which depends on the matching of the mechanical-drill-induced coal breaking and water jet. As shown in Fig. 8, when a is above b , the coal breaking caused by mechanical drill exceeds that of water jet. In this case, the advanced weakened zone could not form and the advanced depressurisation conditions could not be achieved. By contrast, when a is below b , the coal breaking resulted from water jet exceeds that of mechanical drill. In this case, the advanced weakened zone is formed and the confining pressure is fully eliminated, and thus, enabling rapid drilling. In this figure, a is the distance between nozzle 1 and the most distant point of dual-power drill; b is the projection of water jet erosion length. From the aforementioned analysis, it can be seen that the length of slots x is a key parameter for realisation of dual-power drilling, which is derived as follows (The derivation process is

displayed in Appendix A).

$$x = \frac{u_0 d}{\sqrt{\frac{4k^2 R_{DCS}}{\rho_1} \left(1 + \frac{\rho_1 a_1 + 2k_1 R_{DCS}}{\rho_2 a_2}\right)}} \quad (1)$$

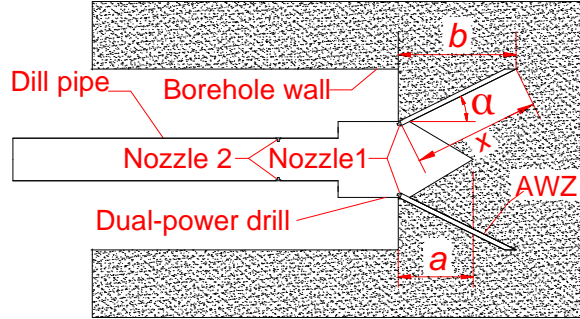


Fig. 8. Dual-power drilling. AWZ = advanced weakened zone

Therefore, the realisation condition of dual-power drilling is

$$b = x \cos \alpha > a \quad (2)$$

Besides, given the guarantee of timely discharge of crushed coal, the flow of water jet should satisfy the following condition:

$$Q \geq \frac{1}{4} u_w \pi (D^2 - d^2) \quad (3)$$

where u_w is water jet velocity, D is diameter of borehole and d is diameter of drill pipe.

3.3 Water jet slotting

Permeability is a vital index for measuring the difficulty of gas flow in coal, which directly influences the effect of gas drainage. Its influencing factors are complex, including its inherent characteristics, confining stress, adsorption property and gas pressure (Zeng et al., 2014; Ghabezloo et al., 2009). The effective stress is a comprehensive expression of confining stress and gas pressure (Jasinge et al., 2011). It can be seen from Fig. 9 that in the process of loading, the increase in effective stress results in rapid decrease in permeability (Li et al., 2014; Meng et al., 2015; Yin et al., 2015). However, the permeability is enhanced substantially at critical effective stress under the condition of unloading. Thus, confining stress relief under a certain gas pressure is an effective measure to improve the permeability and the effect of gas drainage.

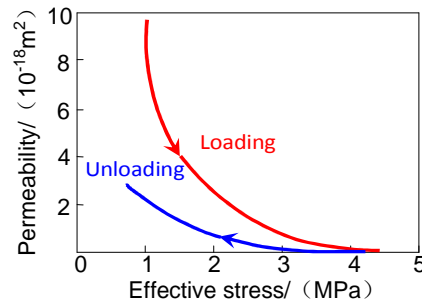


Fig. 9. Relationship between effective stress and permeability.

As shown in Fig. 10a, when a borehole forms, its surrounding stress is re-distributed (Ishida and Uchita, 2000).

Fig. 10. Principle of water jet slotting technique for pressure relief.



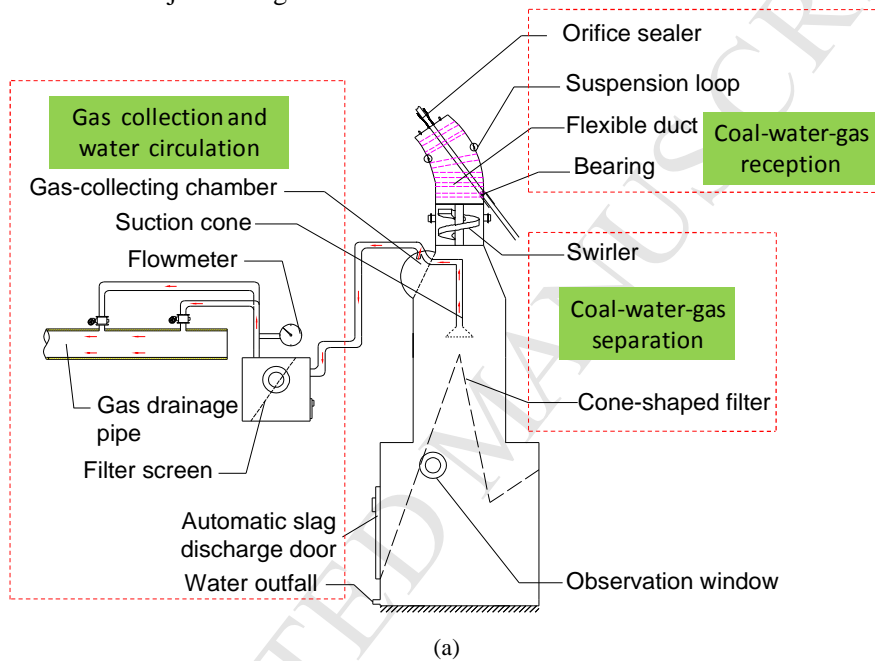
Fig. 11. Dense conventional boreholes.

4 Coal–water–gas separation technique

The ejection of coal and gas from a borehole is such a process that coal collapses in a quasi-equilibrium state and high speed mixture of coal and gas is ejected out between the drill pipe and borehole wall (Ji, 2014; Liu et al., 2014a). It is normally caused by the disturbances, e.g. vibration of drilling borehole. The uncontrollable coal and gas ejection could lead to rapid gas accumulation in underground workplace, posing a threat to the safety of miners. In the process of slotting, the disturbance is caused by the impact of water jet and subsequent erosion. Initially, the distance between the water jet and the borehole wall is extremely small, which results in a great deal of energy dissipation (Zhang et al., 2015). When the disturbance is weak and the coal mass is under a relatively stable state. The crushed coal is gradually discharged and the gas concentration in drilling site is at a normal level ($<1\%$ in volume fraction). As the distance from the nozzle to the coal gradually extends, the coal-breaking performance of water jet improves by a large margin. The disturbance is intensive and the coal mass becomes unstable. The pressure in the borehole will gradually increase, if the crushed coal is not discharged in time and detained in the borehole. When the pressure reaches a critical value, a large amount of coal with gas is ejected out. In this manner, the ejection occurs intermittently. If no measures are taken immediately, the local gas concentration will increase to upper limit, such as the explosion limit on occasion. For sake of safety, slotting will be forced to cease. Moreover, the ejected gas could mix with the roadway airflow and be discharged into the atmosphere. In this sense, coal and gas ejection is also a source of greenhouse gas emission in underground mining. Therefore, measures must be taken to deal with the coal and gas ejection.

In this paper, an instrument of coal–water–gas separation in water jet slotting is developed to solve the aforementioned problem. As shown in Fig. 12, this instrument consists of three sections, namely, coal–water–gas reception, coal–water–gas separation and gas collection/water circulation. With regard to the section of coal–water–gas reception, two basic requirements should be satisfied: The gap between the instrument and borehole should be sealed to avoid the gas leakage at the borehole orifice and the instrument should be adapted to boreholes with various angles and heights. The orifice sealer and flexible duct are designed to meet these two requirements, respectively. Besides, the flexible duct can be fixed at the roadway wall by iron wire or bolt through suspension loop. In general, injecting cement paste is adopted in the conventional method. In this method, the special injection instrument is needed and the gas leakage could occur due to the shrinkage of cement paste. By contrast, the proposed method is more convenient and reliable. The mixture of coal, water and gas flows through the coal–water–gas reception section and enters the coal–water–gas separation section. The principle of swirl

separation is adopted in this instrument (Pisarev and Hoffmann, 2012; Xue et al., 2013). The mixture is swirled by the swirler. Due to the density difference of coal, water and gas, coal concentrates at the inner wall of the instrument and converges at the automatic slag discharge door. The water is mainly penetrated through the cone-shaped filter and flowed out. The water outfall is connected to the water tank in the emulsion pump. Thus, the water is circulated in the whole system, which solves the problem of water accumulation in the lower workplace. The majority of gas is aggregated in the centre of the instrument. With the help of sub-pressure generated by gas drainage pump, the gas is collected by the suction cone and flows into the gas drainage pipe through the filter screen. Besides, the hemisphere-shaped gas-collecting chamber is used to collect the gas near the inner wall. Generally, this instrument is characterised by safe and highly efficient for coal–water–gas separation, which is necessary for smooth implementation of water jet slotting.



(a)



(b)

Fig. 12. Coal–water–gas separation instrument. (a) Cross-section map. (b) Physical map.

5. Sealing–isolation combination technique

After water jet slotting, the borehole should be sealed and gas drainage should be conducted under subpressure conditions. However, the crustal stress re-distributes after the formation of borehole and the coal mass around the borehole deforms accordingly. Generally, the deformation region can be divided into the following three zones based on the state of coal mass: fragmentation zone, plastic zone and elastic zone, which are indicated as I, II and III in Fig. 13 (Hao et al, 2012). In the plastic zone, the deformation is irreversible and many fractures develop, which is unfavourable for the borehole sealing. The radius of this zone can be derived using the following equation (Wang et al, 2008):

$$R = a \left[\frac{(p + c \cot \varphi)(1 - \sin \varphi)}{c \cos \varphi} \right]^{\frac{1 - \sin \varphi}{2 \sin \varphi}} \quad (4)$$

where a is radius of borehole, p is initial crustal stress, c is the cohesive force of coal and φ is internal friction angle.

Generally, the variables p , c and φ are constants for a certain coal/rock. Hence, it can be found from the Eq. (4) that the radius of the plastic zone is proportional to the radius of borehole. In the process of dual-power drilling, the radius enlarges, and thus, the plastic zone is larger than the conventional drilling. Therefore, high-quality sealing is crucial for the recovery of high-concentration gas.

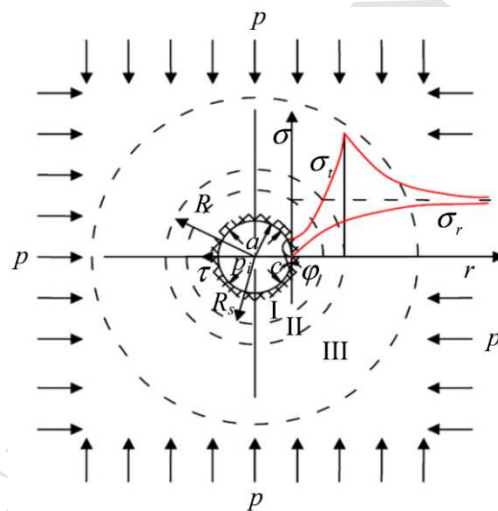


Fig. 13. Stress re-distribution and deformation region around the borehole

Currently, the major materials used for underground borehole sealing are yellow mud, cement-sand grout, high-water material and polyurethane. The high-water material and polyurethane are inappropriate for extensive application in underground sealing due to their exorbitant price. Yellow mud and cement-sand grout are still widely used in approximately 66.6% of China's coal mines (Zhai et al, 2013). However, as shown in Fig. 14, their fatal weakness is shrinkage and cracking after sealing, which leads to serious air leakage under the pressure differences between the exterior and interior sides of the borehole. Besides, flow performances of those two materials are poor. As a result, the fractures far from the borehole are not readily filled. Therefore, it is imperative to develop a new sealing material to achieve high-quality sealing.

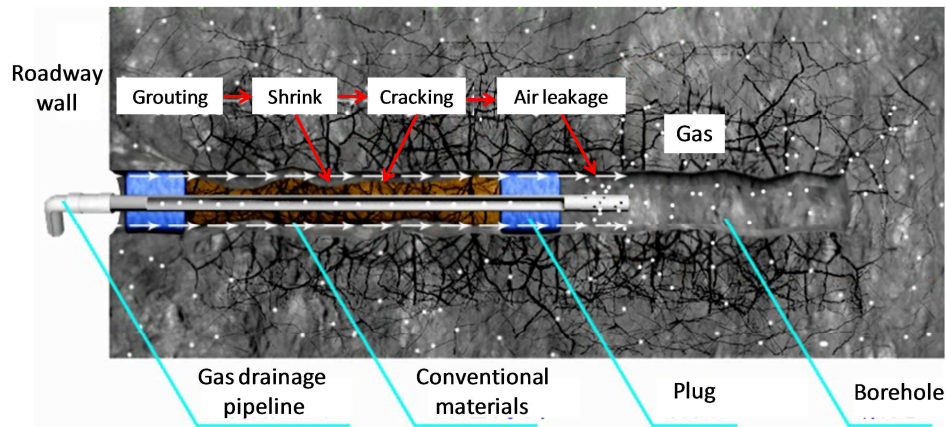


Fig. 14. Borehole sealing by yellow mud and cement-sand grout.

Microencapsulation is a technique of gas, liquid and solid encapsulation using a continuous thin film made of natural or synthetic high-molecular compound, which is applied to maintain the chemical property of the target object (Piva et al., 1997; Masuko et al., 2008). In general, the outer membrane of the capsule directly aggregates on the target object, forming an irregular microcapsule. The average diameter of the microcapsule ranges from $1\mu\text{m}$ to $5000\mu\text{m}$. In this method, the function of the target object could be gradually exerted by outside stimuli and controlled release. To improve the capacity of sealing material, we propose a novel cement-based composite sealing material, which is applied based on the microcapsule technique. The new sealing material is an organic combination of swelling agent and polymer. Besides, some thickening materials and water-retention materials are also added. Initially, the new sealing material is dilute and has good fluidity, which is conducive to grouting. After 5–7 h, the material gradually becomes dense, its volume enlarges and strength improves. After 28 h, the material is solidified into a flexible solid, and the material remains in this state for a long time. As depicted in Fig. 15, the major components of the developed material are cement, water, additive, coupling agent, resin, expansion agent and fibrin. The cement is used to guarantee the compressive strength and control the coagulation time of the material. The function of the dispersant is to ensure uniform mixing of water and cement, which could reduce the usage amount of water. The high-dispersion cement paste is obtained with a mixture of cement, water and dispersant. The polymethyl cellulose solution is selected as the capsule wall material. The liquid microcapsule is obtained by uniform stirring of the swelling agent, cationic flocculant and capsule wall material. The active cement paste is obtained by adding active capsule into the high-disperse cement paste. The water-soluble polymer is the product of polymerisation of water-soluble resin, plasticiser and coupling agent. Finally, the interface recombination of active cement paste and water-soluble polymer produces the new sealing material. The micromorphology of synthesised new sealing material is displayed in Fig. 16.

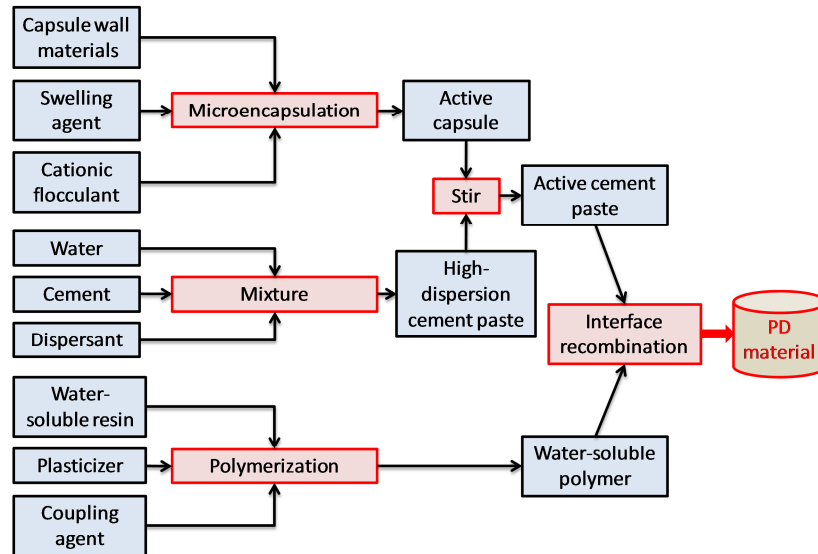


Fig. 15. Technological process of new sealing material development.

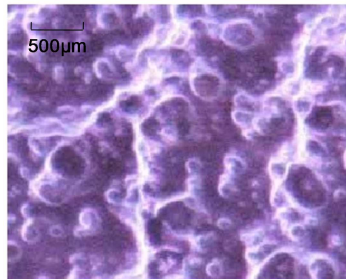


Fig. 16. Micromorphology of new sealing material.

Furthermore, the sealing–isolation combination method is proposed to seal the borehole. The general steps of this method are as follows. Firstly, the slot is generated in the sealing section of borehole. Subsequently, the new sealing material is injected into the sealing section and penetrates into the fractures around the borehole and slot. In this manner, an *airfast wall* forms in the sealing section (Fig. 17). Therefore, the air in the roadway could not flow into the borehole under the subpressure. Thus, the high-concentration gas is guaranteed.

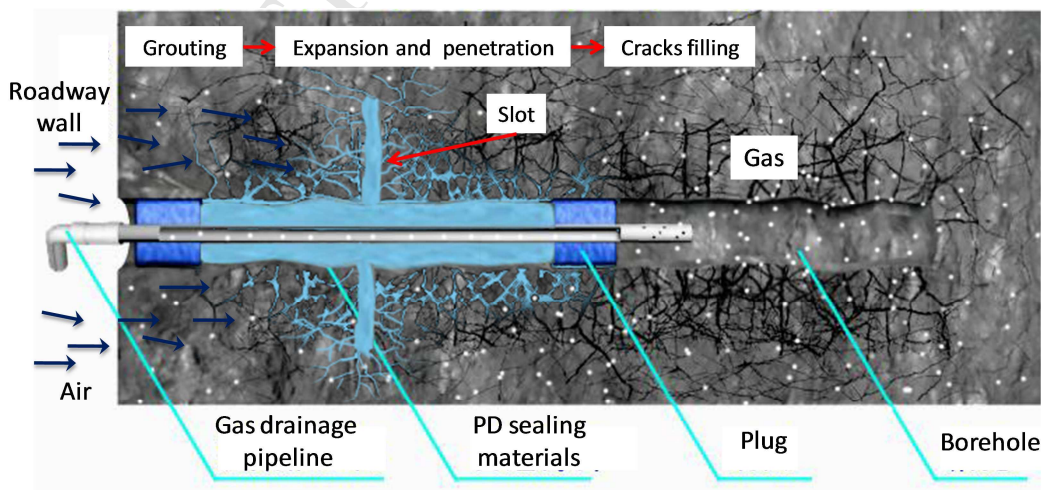


Fig. 17. Sealing–isolation technique.

6 Field test

6.1 Procedures of drilling–slotting–separation–sealing integration techniques

As shown in Fig. 18, obtaining the basic information such as coal seam occurrence conditions before making construction scheme of drilling–slotting–separation–sealing is very important. Once the scheme is determined, the underground construction could be implemented. For one borehole, the subprocedures are as follows: (1) installation of coal–water–gas separation instrument. (2) Drilling with the assistance of water jet. (3) When the borehole crosses the coal seam, water-jet slotting is conducted in the coal section. When the borehole is passes below the coal seam, water-jet slotting is performed outside the safe coal section. Meanwhile, the coal–water–gas separation instrument is used for gas collection and water circulation. (4) When the slotting is completed, the drill pipe is pulled to the sealing section for cutting a slot. (5) The new sealing material is injected and then the gas drainage is conducted. Likewise, other slotted boreholes can be implemented.

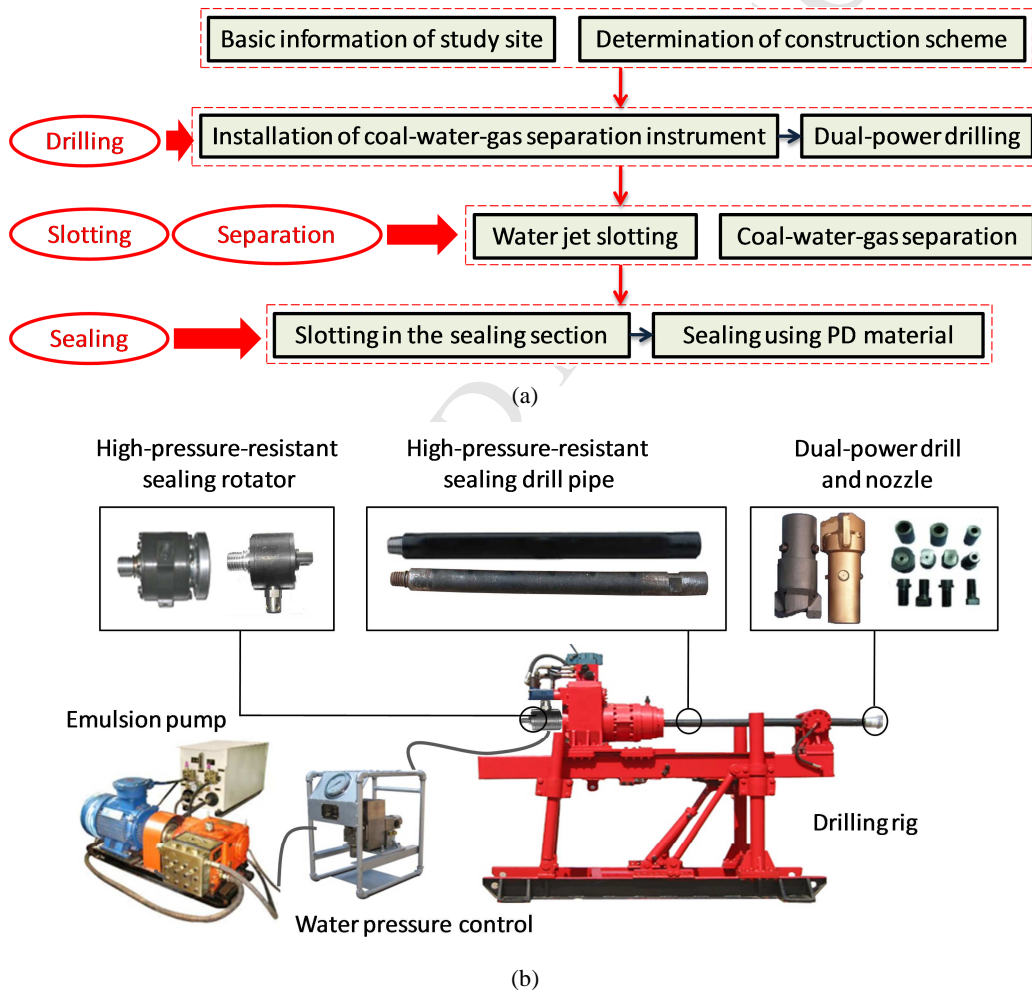


Fig. 18. (a) Steps involved in the drilling–slotting–separation–sealing integrated techniques. (b) Connection of the water-jet slotting system.

6.2 Study site and problems

The Pingdingshan coalfield is located in the western Henan province, China (Fig. 19 a,b). A roadway for gas drainage below the mechanical roadway in mining area no. 13031 of coal mine no. 13 in this coalfield is chosen as

the study site (Fig. 19c). The mining area no. 13031 measures 149.5×421.2 m. The burial depth of the mining area is 587.5–637m. The thickness of coal seam is 5.0~6.7m. The dip angle of coal seam is 8° – 12° . Both the roof and floor are made of sandstone and their thicknesses are 9.8–14.78m and 4.19–11.9m, respectively. The maximum gas pressure and content are 2.5MPa and $15.9\text{m}^3/\text{t}$, respectively, which indicate that the coal seam is at risk of outburst due to the fact that those two values are both over the critical values specified in the State Regulation of Coal and Gas Outburst Prevention and Control of China (Zou et al., 2014b). As shown in Fig. 19d and e, thirteen original cross-measure boreholes were made in every row and the distance of the adjacent rows is 5 m. After gas drainage for approximately 1 year via the cross-measure boreholes, the residual gas content of the coal seam was measured and the maximum content was $12.33\text{m}^3/\text{t}$, which is still higher. During mechanical roadway excavation, the gas dynamic phenomenon is frequent and the gas concentration is approximately 0.8 in volume fraction. Therefore, it is difficult to construct the roadway rapidly and a large amount of gas will be directly discharged into the atmosphere.

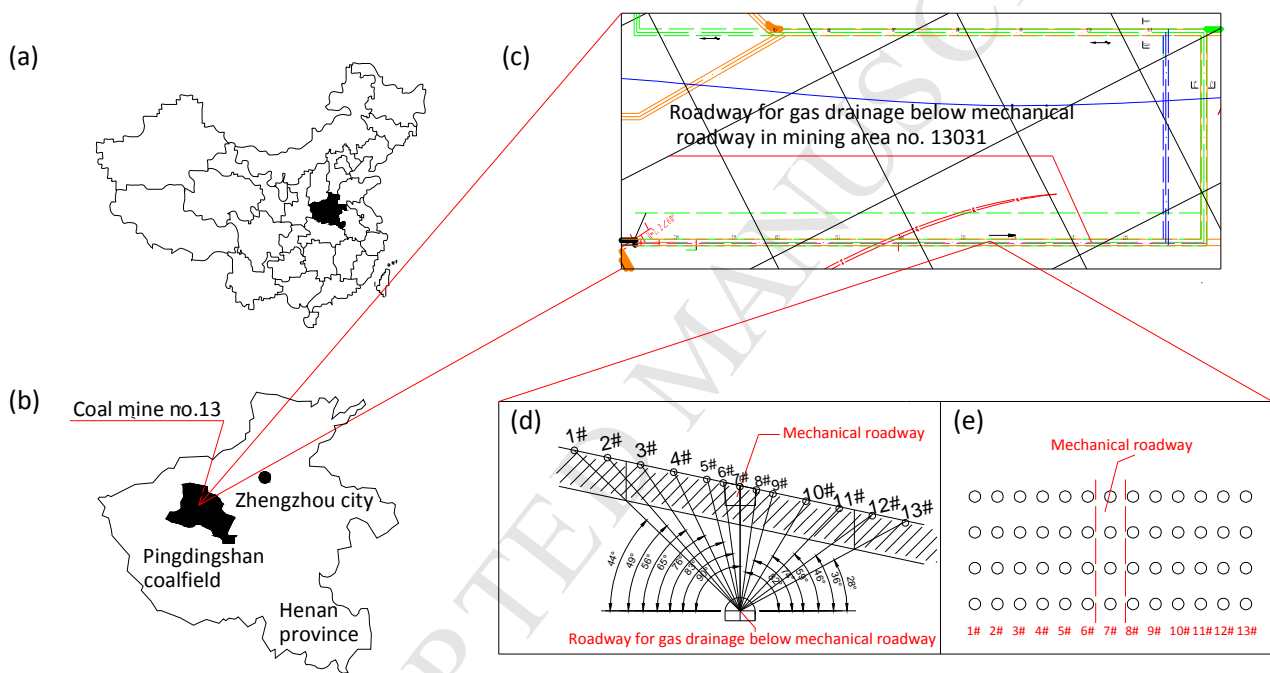


Fig. 19. Study site and original design of boreholes. (a) Location of Henan province in China. (b) Location of Pingdingshan coalfield in Henan province. (c) Roadway layout of mining area no. 13031 and the location of roadway for gas drainage below the mechanical roadway. (d) The original cross-measure borehole arrangement in the roadway for gas drainage below the mechanical roadway (cross-section map). (e) The original cross-measure borehole arrangement in the roadway for gas drainage below the mechanical roadway (plane figure).

6.3 Slotted borehole arrangement and construction

To solve the aforementioned problem, the drilling–slotting–separation–sealing integrated technique was adopted. As shown in Fig. 20, the slotted boreholes were arranged in every row and at the centreline of the adjacent rows. The slotting is only performed in the coal section. It should be noted that only three rows of slotted boreholes are displayed in Fig. 20, as it is unnecessary to go into details of all the slotted boreholes, but we actually drilled 13 rows of boreholes successfully. In this paper, only a row of slotted borehole and three conventional boreholes were elaborated as examples.

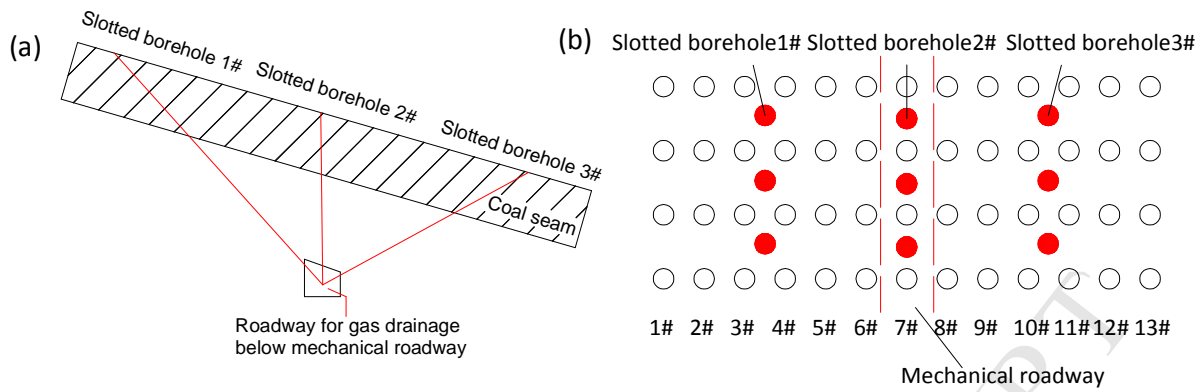


Fig. 20. Slotted boreholes arrangement. (a) Cross-sectional map. (b) Plane figure.

6.4 Variation in gas concentration in drilling site

Four adjacent slotted boreholes are selected to examine the efficiency of the coal–water–gas separation instrument. Two boreholes (designated as SY1 and SY2) were drilled and cut under the protection of the coal–water–gas separation instrument. By contrast, the other two boreholes (designated as WSY1 and WSY2) were drilled and cut without this instrument. The maximum gas concentration at various locations from the slotted boreholes were recorded and depicted in Fig. 21. It can be seen from Fig. 21 that the maximum gas concentration in the two boreholes drilled using the proposed instrument decreases substantially. At these sites, gas collection is significant and safety of the drilling site were guaranteed (It should be noted that the gas, approximately 0.1 in volume fraction, also exists in inlet fresh air.).

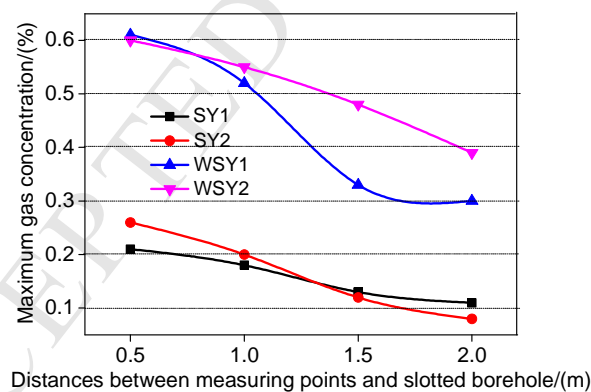


Fig. 21. Maximum gas concentration at various locations from the slotted boreholes.

6.5 Variation in the gas concentration of slotted borehole and the adjacent conventional boreholes

The radical measure of reducing underground gas emission is to drain the gas as soon as possible before beginning coal mining and the drained gas concentration is a fundamental index for the evaluation of the gas-drainage effect. To compare the gas drainage effect of the slotted borehole and conventional borehole, the changes in gas concentration of these two types of boreholes are examined and displayed in Fig. 22. It can be seen from the figure that a high level of gas concentration is maintained in slotted boreholes after gas drainage for more than 40 days. By contrast, the gas concentration of conventional boreholes decreases rapidly. To analyse the gas concentration difference between slotted boreholes and conventional boreholes quantitatively, we calculated their

average gas concentrations (Fig. 22d, C = conventional borehole, S = slotted borehole). The gas concentration in slotted boreholes is estimated to be 1.05–1.91 times larger than that in conventional boreholes. Obviously, the slotted borehole achieves the goal of high-efficiency gas drainage.

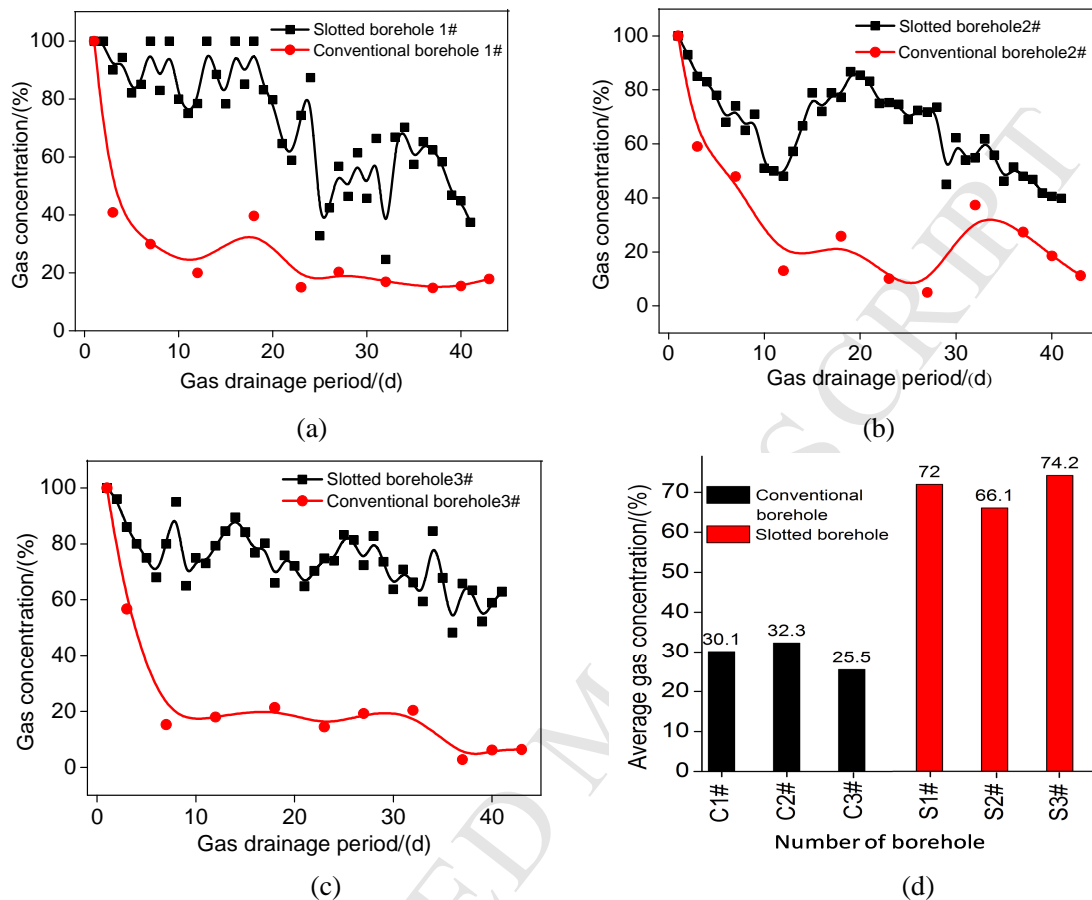


Fig. 22. Changes of gas concentration in slotted and conventional boreholes.

7 Conclusions

In this paper, a modified coal–methane co-exploitation model is proposed to achieve enhanced coal mine methane recovery, which subsequently improves mining safety and reduces coal mine methane emission. Novel integrated techniques of drilling–slotting–separation–sealing were then applied to achieve the desired results. Finally, the field test was conducted to evaluate the efficiency of the proposed method. Primary conclusions of this study are as follows:

(1) The modified coal–methane co-exploitation model is a better choice for improving mining safety and reducing coal mine methane emission. The proposed drilling–slotting–separation–sealing techniques are effective for the exploitation of initial (single) coal seam.

(2) Relief of confining pressure contributes to the substantial decrease in coal compressive strength and significant enhancement of coal permeability. The water jet impact the coal in advance to form the advanced weakening zone and the drilling resistance of mechanical drill lowers with large margin. In this manner, the rapid drilling is realised. Moreover, enhancing the coal permeability improves gas-drainage performance.

(3) Based on the principle of swirl separation, a coal–water–gas separation instrument is developed to eliminate the risk of gas accumulation during slotting and reduce the gas emission from the ventilation air. This instrument includes three components, namely, coal–water–gas reception, coal–water–gas separation and gas collection and water circulation.

(4) Air leakage is a crucial factor influencing high-concentration gas drainage in conventional sealing. Based on the microcapsule technique, a novel cement-based composite sealing material is developed to improve the capacity of sealing material. Furthermore, a novel sealing-isolation technique was also proposed.

(5) Results of field test indicate that the maximum gas concentration in the drilling site substantially decreases after using the coal–water–gas separation instrument. The effect of gas collection is significant and the safety of the drilling site is guaranteed. In addition, the gas concentration in slotted boreholes is 1.05–1.91 times larger than that in conventional boreholes. Thus, the proposed novel integrated techniques achieve the goal of high-efficiency coal bed methane recovery.

Appendix A. Derivation of Eq.(1)

The water jet with high initial velocity u_0 spurts out of the nozzle, forming a discontinuous surface with the surrounding fluid. The fluctuation is induced by the unstable surface, which evolves into vortexes. Consequently, the still air is involved in the water jet. With the further development of the turbulent fluctuation, increasing amounts of still fluid are entrained, which results in the decrease of flow velocity at the water jet edge (Dong, 2005). As shown in Fig. A.1, according to the flow velocity along the axis, the water jet can be divided into three distinct regions, namely, the initial, transitional and main regions (Guha et al., 2011). In most cases, the main region is used in the slotting process owing to the fact that the length of the initial region is extremely short (Beltaos and Rajaratnam, 1973).

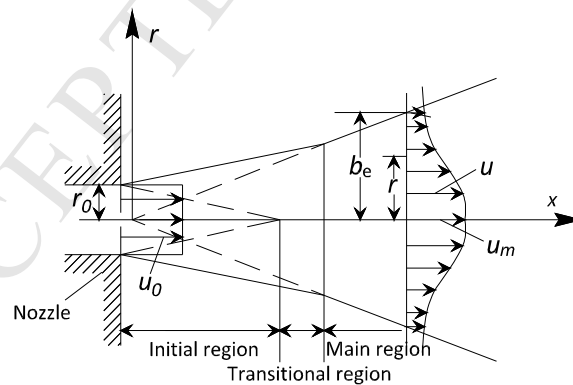


Fig. A.1. Figuration of high-pressure water jet

In the main region, if the viscous tangential force is ignored, the momentum flux (J) conservation in the cross-section of water jet can be derived as follows (Zhang, 2011):

$$J = \int_0^{\infty} \rho u^2 \cdot 2\pi r dr = \rho u_0^2 \pi r_0^2 \quad (\text{A.1})$$

where u is axial velocity; r is cross-sectional radius; ρ is water density; u_0 is the outlet axial velocity and r_0 is outlet radius.

The cross-sectional velocity in the main region is similar (Landa and McClintock, 2004), and is expressed as follows(Dong, 2005):

$$\frac{u}{u_0} = f\left(\frac{r}{b_e}\right) = \exp\left[-\left(\frac{r}{b_e}\right)^2\right] \quad (\text{A.2})$$

where u_m is maximum axial velocity and b_e is the intrinsic semi-thickness of water jet.

It can be obtained by substituting Eq. (A.2) into Eq. (A.1):

$$\int_0^\infty \rho u^2 \cdot 2\pi r dr = \int_0^\infty \rho u_0^2 \exp\left[-2\left(\frac{r}{b_e}\right)^2\right] \cdot 2\pi r dr = \frac{\pi}{2} \rho u_m^2 b_e^2 = \rho u_0^2 \frac{\pi d^2}{4} \quad (\text{A.3})$$

namely,

$$\frac{u_m}{u_0} = \frac{d}{\sqrt{2}b_e} \quad (\text{A.4})$$

where d is outlet diameter, $d=2r_0$.

Assuming that the thickness of water jet extends linearly namely $b_e = kx$ (Lu et al., 2015), the following equation can be obtained:

$$\frac{u_m}{u_0} = \frac{1}{\sqrt{2}k} \left(\frac{d}{x}\right) \quad (\text{A.5})$$

It can be concluded from Eq. (A.4) that the rules of water jet velocity attenuation accords with inverse function.

Coal/rock breaking by water jet is a complicated process and affected by various factors, which mainly includes the properties of coal/rock (structural characteristic, heterogeneity, wave resistance and property of elasticity and strength) and water jet (impact pressure, standoff distance, transverse speed and impact angle) (Zou et al., 2014a). For simplicity, the property of coal/rock is represented by dynamic strength and wave resistance and the property of water jet is represented by impact pressure, impact velocity and wave resistance. The breaking criterion that coal/rock breaking occurs when the impact pressure is above the dynamic strength of coal is adopted (Wang et al. 2011). Thus, the critical velocity of coal/rock breaking can be derived using the internal relationship between water jet and coal/rock.

Water and coal/rock are both compressive. When the water jet impacts coal/rock, the velocity jump of mass point can be expressed as:

$$u_2 = V_{\text{impact}} - u_1 \quad (\text{A.6})$$

where u_1 is the velocity jump of mass point in water jet; u_2 is the velocity jump of mass point in coal/rock; V_{impact} is impact velocity.

The relationship between velocity of mass point in coal/rock and impact pressure can be expressed as follows (Xu and Yu, 1984):

$$P = \rho_2 u_2 a_2 \left(1 + k_2 \frac{u_2}{a_2}\right) = \rho_2 (V_{\text{impact}} - u_1) a_2 \left(1 + k_2 \frac{V_{\text{impact}} - u_1}{a_2}\right) \quad (\text{A.7})$$

where P is the maximum impact of water jet; ρ_2 is coal/rock density; a_2 is wave velocity in coal/rock and k_2 is impact constant of coal/rock.

The pressure of water jet P_j can be calculated by

$$P_j = \rho_1 u_1 a_1 \left(1 + k_1 \frac{u_1}{a_1} \right) \quad (\text{A.8})$$

where ρ_1 is water density; a_1 is wave velocity in still water under atmospheric pressure and k_1 is water jet coefficient.

It can be derived from the equilibrium condition at boundary layer of solid and liquid (Hsu et al., 2013).

$$\rho_2 (V_{\text{impact}} - u_1) a_2 \left(1 + k_2 \frac{V_{\text{impact}} - u_1}{a_1} \right) = \rho_1 u_1 a_1 \left(1 + k_1 \frac{u_1}{a_1} \right) \quad (\text{A.9})$$

The dynamic compressive strength of coal/rock R_{DCS} can be obtained from the aforementioned breaking criterion.

$$R_{DCS} \leq \frac{\rho_1 u_1^2}{2} \quad (\text{A.10})$$

The impact velocity V_{impact} for initial coal/rock breaking can be derived by combining Eqs. (8) and (9).

$$V_{\text{impact}} \geq \sqrt{\frac{2R_{DCS}}{\rho_1} \left(1 + \frac{\rho_1 a_1 + 2k_1 R_{DCS}}{\rho_2 a_2} \right)} \quad (\text{A.11})$$

Eq. (10) shows that the impact velocity V_{impact} of initial coal/rock breaking correlates with the property of coal/rock (dynamic compressive strength R_{DCS} , density and wave velocity) and water jet (density and wave velocity).

If $V_{\text{impact}} = u_m$, we can obtain the length of slot x .

$$x = \frac{u_0 d}{\sqrt{\frac{4k^2 R_{DCS}}{\rho_1} \left(1 + \frac{\rho_1 a_1 + 2k_1 R_{DCS}}{\rho_2 a_2} \right)}} \quad (\text{A.12})$$

Acknowledgements

This work is supported by the National Science and Technology Support Program (No. 2012BAK04B07), State Key Basic Research Program of China (No.2011CB201205), and National Natural Science Foundation of China (No.51474211).

References

- Al-Amin, A.Q., Kari, F., 2013. Global warming and climate change: prospects and challenges toward long-term policies in Bangladesh. *Int. J. Global. Warm.* 5,67-83.
- Bamberger, I., Stieger, J., Buchmann, N., Eugster, W., 2014. Spatial variability of methane: Attributing atmospheric concentrations to emissions. *Environ. Pollut.* 190,65-74.
- Baris, K., 2013. Assessing ventilation air methane (VAM) mitigation and utilization opportunities: A case study at

- Kozlu Mine, Turkey. *Energy Sustain Dev.* 17,13-23.
- Beltaos, S., Rajaratnam, N., 1973. Plane turbulent impinging jets. *J. Hydraul. Res.* 11,29–59.
- BP (2014) Annual energy outlook with projections to 2040. U.S. Energy Information Administration
- Budzianowski, W.M., 2012. Value-added carbon management technologies for low CO₂ intensive carbon-based energy vectors. *Energy* 41,280-297.
- Budzianowski, W.M., 2013. Modelling of CO₂ content in the atmosphere until 2300: influence of energy intensity of gross domestic product and carbon intensity of energy. *Int. J. Global. Warm.* 41,280-297.
- Chen., J, Jiang., D.Y., Ren, S., Yang, C.H., 2015. Comparison of the characteristics of rock salt exposed to loading and unloading of confining pressures. *Acta Geotech.* DOI 10.1007/s11440-015-0369-9.
- Cheng, Y.P., Wang, L., Zhang, X.L., 2011. Environmental impact of coal mine methane emissions and responding strategies in China. *Int. J. of Greenh. Gas Con.* 5,157–166.
- Dong, Z.Y., 2005. *Waterjet Mechanics*. Science Press. Beijing.
- Ghabezloo, A., Sulem, J., Guedon, S., Martineau, F., 2009. Effective stress law for the permeability of a limestone. *Int. J. Rock Mech. Min.* 46,297–306.
- Guha, A., Barron, R.M., Balachandar, R., 2011. An experimental and numerical study of water jet cleaning process. *J. Mater. Process. Tech.* 1,610–618.
- Gunter, W.D, Gentzis, T., Rottenfusser, B.A., Richardson, R.J.H., 1997. Deep coalbed methane in Alberta, Canada: A fuel resource with the potential of zero greenhouse gas emissions. *Energ. Convers. Manage.* 38,217-222.
- Guo, H., Yuan, L., Shen, B.T., Qu, Q.D., Xue, J.H., 2012. Mining-induced strata stress changes, fractures and gas flow dynamics in multi-seam longwall mining. *Int. J. Rock Mech. Min.* 54,129-139.
- Hao, Z.Y., Li, B.Q., Gao, Y.B., Cheng, Y.Y., 2012. Establishment and application of drilling sealing model in the spherical grouting mode based on the loosening-circle theory. *Int. J. Min. Sci. Technol.* 22,895-898.
- Hao, Z.Y., Zhou, C., Li, B.Q., Pang, Y., Li, Z.W., 2014. Pressure-relief and permeability-increase technology of high liquid–solid coupling blast and its application. *Int. J. Min. Sci. Technol.* 24,45-49.
- He, X.Q., Li, S., 2012. Status and future tasks of coal mining safety in China. *Safety Sci.* 50,894-898.
- Hook, M., Tang, X., 2013. Depletion of fossil fuels and anthropogenic climate change—A review. *Energ. Policy* 52,797-809.
- Hsu, C.Y, Liang, C.C., Teng, T.L, Nguyen, A.T., 2013. A numerical study on high-speed water jet impact. *Ocean Eng.* 72,98–106.
- Huang, B.X., Liu, C.Y., Fu, J.H., Guan, H., 2011. Hydraulic fracturing after water pressure control blasting for increased fracturing. *Int. J. Rock Mech. Min.* 48,976–983.
- IPCC, 2007. *Climate Change 2007: Synthesis Report*. Contribution of Working Groups I, II and III to the Fourth Assessment Report of the Intergovernmental Panel on Climate Change. International Panel on Climate Change (IPCC), Geneva, Switzerland.
- Ishida, T., Uchida, Y., 2009. Strain monitoring of borehole diameter changes in heterogeneous jointed wall rock with chamber excavation; estimation of stress redistribution. *Eng. Geol.* 56,63–74.
- Jasinge, D., Ranjith, P.G., Choi, S.K., 2011. Effects of effective stress changes on permeability of latrobe valley

brown coal. *Fuel* 90,1292–1300.

- Ji, Q.H., 2014. Research and application of auger-air drilling and sieve tube borehole protection in soft outburst-prone coal seams. *Proc. Eng.* 73,283-288.
- Karacan, C., Ruiz, F.A., Cotè, M., Phipps, S., 2011. Coal mine methane: A review of capture and utilization practices with benefits to mining safety and to greenhouse gas reduction. *Int. J. Coal Geol.* 86,121-156.
- Karakurt, I., Aydin, G., Aydiner, K., 2011. Mine ventilation air methane as a sustainable energy source. *Renew. Sust. Energ. Rev.* 15,1042-1049.
- Kiyama, T., Nishimoto, S., Fujioka, M., Ziqiu, Xue, Z.Q., Ishijima, Y., Pan, Z.J., Connell, L.D. 2011. Coal swelling strain and permeability change with injecting liquid/supercritical CO₂ and N₂ at stress-constrained conditions. *Int. J. Coal Geol.* 85,56-64.
- Lashof, D.A., Ahuja, D.R., 1990. Relative contributions of greenhouse gas emissions to global warming. *Nature* 344,529-531.
- Landa, P.S., McClintock, P.V.E., 2004. Development of turbulence in subsonic submerged jets. *Phys. Rep.* 397,1–62.
- Lama, R.D., Bodziony, J., 1998. Management of outburst in underground coal mines. *Int. J. Coal Geol.* 35,83-115.
- Li, Q.G., Lin, B.Q., Zhai, C., 2015a. A new technique for preventing and controlling coal and gas outburst hazard with pulse hydraulic fracturing: a case study in Yuwu coal mine, China. *Nat. Hazards* 75,2931-2946.
- Li, W., Younger, P.L., Cheng, Y.P., Zhang, B.Y., Zhou, H.X., Liu, Q.Q., Dai, T., Kong, S.L., Jin, K., Yang, Q.L. 2015b. Addressing the CO₂ emissions of the world's largest coal producer and consumer: Lessons from the Haishiwan Coalfield, China. *Energy* 80,400–413.
- Li, W., Zhu, J.T., Cheng, Y.P., Lu, S.Q., 2014a. Evaluation of coal swelling-controlled CO₂ diffusion processes. *Greenh.Gases* 4,131–139.
- Li, Y., Tang, D.Z., Xu, H., Meng, Y.J., Li, J.Q., 2014b. Experimental research on coal permeability: The roles of effective stress and gas slippage. *J. Nat. Gas Sci. Eng.* 21,581–488.
- Lin, B.Q., Dai, H.M., Wang, C.Q., Li, Q.Z., Wang, K., Zheng, Y.Z., 2014. Combustion characteristics of low concentration coal mine methane in divergent porous media burner. *Int. J. Min. Sci. Technol.* 24,671-677.
- Liu, C., Zhou, F.B., Yang, K.K., Xiao, X., Liu, Y.K., 2014a. Failure analysis of borehole liners in soft coal seam for gas drainage. *Eng. Fail. Anal.* 42,274-283.
- Liu, H.B., Liu, H., Cheng, Y.P., 2014b. The elimination of coal and gas outburst disasters by ultrathin protective seam drilling combined with stress-relief gas drainage in Xinggong coalfield. *J. Nat. Gas Sci. Eng.* 21,837–844.
- Liu, H.Y., Cheng, Y.P., Chen, H.D., Mou, J.H., Kong, S.L., 2013. Characteristics of mining gas channel expansion in the remote overlying strata and its control of gas flow. *Int. J. Min. Sci. Technol.* 23,481-487.
- Liu, Q.Q., Cheng, Y.P., Yuan, L., Tong, B., Kong, S.L., Zhang, R., 2014c. CMM capture engineering challenges and characteristics of in-situ stress distribution in deep level of Huainan coalfield. *J. Nat. Gas Sci. Eng.* 20,328–336.
- Liu, Y.W., Wang, Q., Chen, W.X., Liu, M.J., Hani, M., 2014d. Preferential adsorption behaviour of CH₄ and CO₂ on high-rank coal from Qinshui Basin, China. *Int. J. Min. Reclam. Env.* DOI: 10.1080/17480930.2014.964040.

- Liu, T., Lin, B.Q., Zou, Q.L., 2015. Investigation on mechanical properties and damage evolution of coal after hydraulic slotting. *J. Nat. Gas Sci. Eng.* 24, 489-499.
- Lu, T.K., Yu, H., Dai, Y.H., 2010. Longhole waterjet rotary cutting for in-seam cross panel methane drainage. *Int. J. Min. Sci. Technol.* 20,378-383.
- Lu, Y.Y., Huang, F., Liu, X.C., Ao, X., 2015. On the failure pattern of sandstone impacted by high-velocity water jet. *Int. J. Impact Eng.* 76,67-74.
- Masuko, M., Sato, H., Suzuki, A., Kurosawa, O., 2008., Prevention of oxidative degradation of ZnDTP by microcapsulation and verification of its antiwear performance. *Tribol. Int.* 41,1097-1102.
- Mazumder, S., Wolf, K.H., 2008. Differential swelling and permeability change of coal in response to CO₂ injection for ECBM. *Int. J. Coal Geol.* 74,123-138.
- Mazzotti, M., Pini, R., Storti, G., 2009. Enhanced coalbed methane recovery. *J. Supercrit. Fluids* 47,619-627.
- Meng, J.Q., Nie, B.S., Zhao, B., Ma, Y.C., 2015. Study on law of raw coal seepage during loading process at different gas pressures. *Int. J. Min. Sci. Technol.* 25,31-35.
- Nejat, P., Jomehzadeh, F., Taheri, M.M., Gohari, M., Majid, M.Z.A., 2015. A global review of energy consumption, CO₂ emissions and policy in the residential sector (with an overview of the top ten CO₂ emitting countries). *Renew. Sustain. Energ. Rev.* 43,843-862.
- Ni, G.H., Lin, B.Q., Zhai, C., Li, Q.G., Peng, S., Li, X.Z., 2014. Kinetic characteristics of coal gas desorption based on the pulsating injection. *Int. J. Min. Sci. Technol.* 24,631-636.
- Pan, J.N., Zhu, H.T., Hou, Q.L., Wang, H.C., Wang, S., 2015. Macromolecular and pore structures of Chinese tectonically deformed coal studied by atomic force microscopy. *Fuel* 139,94-107.
- Pan, Z.J., Connell, L.D., 2011. Impact of coal seam as interlayer on CO₂ storage in saline aquifers: A reservoir simulation study. *Int. J. Greenh.Gas Con.* 5,99-114.
- Pisarev, G.I., Hoffmann, A.C., 2012. Effect of the 'end of the vortex' phenomenon on the particle motion and separation in a swirl tube separator. *Powder Technol.* 222,101-107.
- Piva, A., Anfossi, P., Meola, E., Pietri, A., Panciroli, A., Bertuzzi, T., Formigoni, A., 1997. Effect of microcapsulation on absorption processes in the pig. *Livest. Prod. Sci.* 51,53-61.
- Qin, Y., 2008. Mechanism of CO₂ enhanced CBM recovery in China: a review. *Int. J. Min. Sci. Technol.* 18,406-412.
- Qu., H.Y., Liu, J.S., Chen, Z.W., Wang, J.G., Pan, Z.J., Connell, L., Elsworth, D., 2012. Complex evolution of coal permeability during CO₂ injection under variable temperatures. *Int. J. Greenh.Gas Con.* 9,281-293.
- Rodrigues, C., Dinis, C.R., Dinis, M.A., 2013. Unconventional coal reservoir for CO₂ safe geological sequestration. *Int. J. Global Warm.* 5,46-66.
- Saghafi, A., 2010. Potential for ECBM and CO₂ storage in mixed gas Australian coals. *Int. J. Coal Geol.* 62,240-251.
- Sander, R., Connell, L.D., 2012. Methodology for the economic assessment of enhanced coal mine methane drainage (ECMM) as a fugitive emissions reduction strategy. *Int. J. Greenh.Gas Con.* 8,34-44.
- Sander, R., Connell, L.D., 2014. A probabilistic assessment of enhanced coal mine methane drainage (ECMM) as a fugitive emission reduction strategy for open cut coalmines. *Int. J. Coal Geol.* 131,288-303.

- Shealy, M., Dorian, J.R., 2010. Growing Chinese coal use: Dramatic resource and environmental implications. *Energ. Policy* 38,2116-2122.
- Sitharam, T.G., 1999. Micromechanical modeling of granular materials: effect of confining pressure on mechanical behaviour. *Mech. Mater.* 31,653-665.
- Sobczyk, J., 2014. A comparison of the influence of adsorbed gases on gas stresses leading to coal and gas outburst. *Fuel* 115,288-294.
- Su, S., Beath, A., Guo, H., Mallett, C., 2005. An assessment of mine methane mitigation and utilisation technologies. *Prog. Energ. Combust. Sci.* 31,123-170.
- Su, S., Han, J.Y., Wu, J.Y., Li, H.J., Worrall, R., Guo, H., Sun, X., Liu, W.G., 2011. Fugitive coal mine methane emissions at five mining areas in China. *Atmos. Environment* 45,2220-2232.
- Suchowerska, A.M., Merifield, R.S., Carter, J.P., 2013. Vertical stress changes in multi-seam mining under supercritical longwall panels. *Int. J. Rock Mech. Min.* 61,306-320.
- Warmuzinski, K., 2008. Harnessing methane emissions from coal mining. *Process Saf. Environ.* 86,315-320.
- Wang, E.Y., He, X.Q., Wei, J.P., Nie, B.S., Song, D.Z., 2011. Electromagnetic emission graded warning model and its applications against coal rock dynamic collapses. *Int. J. Rock Mech. Min.* 48,556-564.
- Wang, F.T., Ren, T., Tu S.H., Hungerford, F., Aziz, N., 2012a. Implementation of underground longhole directional drilling technology for greenhouse gas mitigation in Chinese coal mines. *Int. J. Greenh. Gas Con.* 11,290-303.
- Wang, L., Cheng, Y.P., 2012b. Drainage and utilization of Chinese coal mine methane with a coal-methane co-exploitation model: Analysis and projections. *Resources Policy* 37,315-321.
- Wang, L., Cheng, Y.P., Liu, H.Y., 2014. An analysis of fatal gas accidents in Chinese coal mines. *Safety Sci.* 62,107-113.
- Wang, W.C., Li, X.Z., Lin, B.Q., Zhai, C., 2015. Pulsating hydraulic fracturing technology in low permeability coal seams. *Int. J. Min. Sci. Tech.* 25,681-685.
- Wang, Z.T., Zhou, H.Q., Xie, Y.S., 2008. *Mine rock mechanics*. China University of Mining and Technology Press. Xuzhou.
- White, C.M., Smith, D.H., Jones, K.L., Goodman, A.L., Jikich, S.A., LaCount, R.B., DuBose, S.B., Ozdemir, E., Morsi, B.I., Schroeder, K.T., 2005. Sequestration of carbon dioxide in coal with enhanced coalbed methane recovery-A review. *Energ. Fuel.* 19,659-724.
- Xu X.H., Yu J (1984) *Theory of Rock Fragmentation*. Coal Industry Press. Beijing.
- Xue, Y.P., Arjomandi, M., Kelso, R., 2013. The working principle of a vortex tube. *Int. J. Refrig.* 36,1730-1740.
- Yan, F.Z., Lin, B.Q., Zhu, C.J., Shen, C.M., Zou, Q.L., Guo, C., Liu, T., 2015. A novel ECBM extraction technology based on the integration of hydraulic slotting and hydraulic fracturing. *J. Nat. Gas Sci. Eng.* 22,571-579.
- Yang, W., Lin, B.Q., Qu, Y.A., Li, Z.W., Zhai, C., Jia, L.L., Zhao, W.Q., 2011a. Stress evolution with time and space during mining of a coal seam. *Int. J. Rock Mech. Min.* 48,1145-1152.
- Yang, W., Lin, B.Q., Qu, Y.A., Zhao, S., Zhai, C., Jia, L.L., Zhao, W.Q., 2011b. Mechanism of strata deformation under protective seam and its application for relieved methane control. *Int. J. Coal Geol.* 85,300-306.
- Yang, W., Lin, B.Q., Yang, Q., Zhai, C., 2014. Stress redistribution of longwall mining stope and gas control of

- multi-layer coal seams. *Inter. J. Rock Mech. Min.* 72,8-15.
- Yin, G.Z., Jiang, C.B., Wang, J.G., Xu, J., 2015. Geomechanical and flow properties of coal from loading axial stress and unloading confining pressure tests. *Int. J. Rock Mechan. Min.* 76,155-161.
- Yu, H.G., Jing, R.X., Wang, P.P., Chen, L.H., Yang, Y.J., 2014. Preferential adsorption behaviour of CH₄ and CO₂ on high-rank coal from Qinshui Basin, China. *Int. J. Min. Sci. Tech.* 24,491-497.
- Yuan, L., 2009. Theory of pressure relieved gas extraction and techniques system of integrated coal production and gas extraction. *J. China Coal Soc.* 34,5-12.
- Yusuf, R.O., Noor, Z.Z., Abba, A.H., Hassan, M.A.A., Din, M.F.M., 2012. Methane emission by sectors: A comprehensive review of emission sources and mitigation methods. *Renew. Sust. Energ. Rev.* 16,5059-5070.
- Zeng, Z.J., Li, X.C., Shi, L., Bai, B., Fang, Z.M., Wang, Y., 2014. Experimental study of the laws between the effective confining pressure and mudstone permeability. *Energ. Pro.* 63,5654-5663.
- Zhai, C., Xiang, X.W., Yu, X., Peng, S., Ni, G.H., Li, M., 2013. Sealing performance of flexible gel sealing material of gas drainage borehole. *J. China U. Min.Tech.* 42,982-988.
- Zhao, G., Chen, S., 2014. Greenhouse gas emissions reduction in China by cleaner coal technology towards 2020. *Energ. Strategy Rev.* <http://dx.doi.org/10.1016/j.esr.2014.08.001>.
- Zhang, J.G., 2011. Research on primary parameters of high pressure water jet during rock cross-cut coal uncovering. *Journal of Chongqing University* 34,117-121.
- Zhang, S.Z., Johansen, K.D., Bernad, P.L., Kiil, S., 2015. Rain erosion of wind turbine blade coatings using discrete water jets: Effects of water cushioning, substrate geometry, impact distance, and coating properties. *Wear* 328-329,140-148
- Zhou, H.X., Zhang, R., Cheng, Y.P., Dai, H., Ge, C.G., Chen, J.X., 2015. Methane and coal exploitation strategy of highly outburst-prone coal seam configurations. *J. Nat. Gas Sci. Eng.* 23,63-69.
- Zou, Q.L., Lin, B.Q., Liu, T., Zhou, Y., Zhang, Z., Yan, F.Z., 2014a. Variation of methane adsorption property of coal after the treatment of hydraulic slotting and methane pre-drainage: A case study. *J. Nat. Gas Sci. Eng.* 20,396-406.
- Zou, Q.L., Lin, B.Q., Liang, J.Y., Liu, T., Zhou, Y., Yan, F.Z., Zhu, C.J. 2014b. Variation in the pore structure of coal after hydraulic slotting and gas drainage. *Adsorpt. Sci. Technol.* 32,647-666.

1. A modified coal–methane co-exploitation model is proposed to achieve enhanced coal mine methane recovery.
2. Rapid drilling could be realized via water jet impact on the coal/rock mass in advance to form advanced weakening zone.
3. Based on swirl separation, a coal–water–gas separation instrument is developed to eliminate the risk of gas accumulation during slotting.
4. Based on the microcapsule technique, a novel cement-based composite sealing material is developed to improve the performance of sealing material.